PROCEEDINGS A

rspa.royalsocietypublishing.org

Research

Cite this article: Erbaş B, Kaplunov J, Nolde E, Palsü M. 2018 Composite wave models for elastic plates. *Proc. R. Soc. A* **474**: 20180103. http://dx.doi.org/10.1098/rspa.2018.0103

Received: 14 February 2018
Accepted: 16 May 2018

Subject Areas:
applied mathematics, mechanics

Keywords:
elastic plate, composite, asymptotic, Rayleigh wave, hyperbolic equation

Author for correspondence:
Julius Kaplunov
e-mail: j.kaplunov@keele.ac.uk

Composite wave models for elastic plates

Barış Erbaş [1], Julius Kaplunov[2], Evgeniya Nolde[3] and Melike Palsü[1]

[1]Anadolu University, Department of Mathematics, Yunus Emre Campus, 26470 Eskisehir, Turkey
[2]School of Computing and Mathematics, Keele University, Keele ST5 5BG, UK
[3]Department of Mathematics, CEDPS, Brunel University London, Uxbridge UB8 3PH, UK

JK, 0000-0001-7505-4546

The long-term challenge of formulating an asymptotically motivated wave theory for elastic plates is addressed. Composite two-dimensional models merging the leading or higher-order parabolic equations for plate bending and the hyperbolic equation for the Rayleigh surface wave are constructed. Analysis of numerical examples shows that the proposed approach is robust not only at low- and high-frequency limits but also over the intermediate frequency range.

1. Introduction

A substantial fresh interest in the mechanics of thin elastic structures, inspired by the demands of modern advanced technologies, is strongly focused on modelling of microscale phenomena, e.g. see recent publications [1–5]. At the same time, the long-standing problem concerned with the derivation of a two-dimensional (2D) hyperbolic plate theory supporting an asymptotically consistent short-wave behaviour is not yet solved even in the context of linear isotropic elasticity. The classical Kirchhoff plate theory is governed by a fourth-order equation, which may be classified as parabolic [6]. As a consequence, it does not predict a finite wave speed limit resulting in a formal violation of the causality principle. However, as the leading long-wave low-frequency approximation of three-dimensional (3D) equations in elasticity (e.g. [7–9]), the Kirchhoff equation is not assumed to be

THE ROYAL SOCIETY PUBLISHING

valid near wavefronts dominated by short-wave high-frequency patterns. The causality of long-wave models was also discussed for periodic media, including discrete chains [10–12]. In fact, as was demonstrated in [13], the asymptotic methodologies underlying thin and periodic structures appear to have a lot in common.

Refined ad hoc plate formulations, including Timoshenko–Reissner–Mindlin-type theories as well as numerous later considerations, often start from hyperbolic equations; see general reference works [14,15] and also papers [16,17]. Simultaneously, the hyperbolicity of all of them is rather a type of a side effect related to incorporating certain long-wave corrections like shear deformation and rotation inertia, but not the result of adapting a proper short-wavelength asymptotic limit. The wave speeds within various versions of refined ad hoc theories may either coincide with bulk and surface wave speeds in a 3D elastic solid or take slightly different values, see [14]. The heuristic nature of the arguments supporting existing hyperbolic formulations is appreciated in [18], combining them with a long-wave variational-asymptotic approach.

The main challenge of constructing asymptotically consistent 2D hyperbolic theories is that the equations of the short-wave approximations in question generally have to retain derivatives with respect to the third (thickness) variable. In particular, for a semi-infinite thin shell of revolution subject to edge impact loading, these equations take the form of plane and anti-plane problems in elasticity over the transverse cross section of the shell, see [8] and also the specialized monograph [19]. Obviously, plane and anti-plane problems preserve the correct values of 3D bulk wave speeds. Their solutions may be matched with those of the Kirchhoff–Love theory of shells, which is valid outside wavefront vicinities.

A new prospect for deriving 2D hyperbolic equations has recently arisen due to the development of the asymptotic hyperbolic–elliptic model for the surface Rayleigh wave, see [20,21] and references therein. It is very crucial for our purposes that it operates with an explicit 2D wave equation along the surface. In this case, 3D 'static' elliptic equations have to be solved over the interior. The model is derived by perturbing the inhomogeneous equations in elasticity around the Rayleigh wave eigen-solution orginally obtained in [22,23]. We also mention more recent publications [24,25] dealing with the free surface waves of an arbitrary profile. Although the aforementioned model assumes near-resonant loading, it also allows one to determine the Rayleigh wave contribution to the overall response in the case of a more general excitation. It was successfully implemented for a number of dynamic problems for point and moving surface sources [26–28].

In this paper, we attempt to establish 2D composite hyperbolic equations for an elastic plate using the Kirchhoff or refined asymptotic plate equations along with the Rayleigh wave equation; see [29,30] regarding the idea of composite equations incorporating both long- and short-wave limiting forms, for which a typical wavelength is much greater or smaller than the plate thickness. We restrict ourselves to surface loading, when bending and Rayleigh waves are seemingly of the most importance. In contrast with examples in [29], we do not expect from the very beginning to arrive at uniformly valid composite equations. The point is that over the intermediate range, for which a wavelength is of order of the thickness, a plate demonstrates essentially 3D behaviour, which does not allow any asymptotic dimension reduction.

The paper is organized as follows. The governing equations are written down in §2. In this section, the Kirchhoff plate equation as well as its asymptotic refinement are rewritten through surface displacements. Also, the 2D hyperbolic equation for the Rayleigh wave, initially derived for the surface wave potentials, is presented in terms of displacements. It is worth noting that the right-hand side of the hyperbolic equation for the vertical displacement contains a pseudo-differential operator acting on prescribed normal surface stresses. In §3, we begin with an analysis of the dispersion relations. Along with the simplest composite relation based on the Kirchhoff equation, we also suggest a more sophisticated one corresponding to the refined plate equation. The composite dispersion relations are tested by comparison with the results of the numerical evaluation of the fundamental Rayleigh–Lamb antisymmetric mode. In §4, using a preliminary insight from the previous section, we establish hyperbolic composite equations starting, again, from both the Kirchhoff and refined plate theories combined with the Rayleigh wave model.

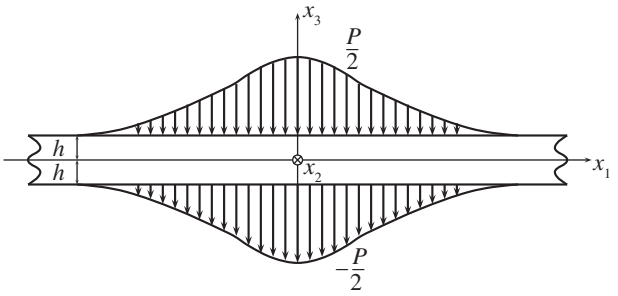

Figure 1. Antisymmetric deformation of an elastic layer under surface loading.

Leading-order composite equations are presented in terms of both vertical and horizontal displacements. In addition, a refined composite equation is obtained for vertical displacement. In §5, the solutions of the composite equations are compared with those of the associated plane strain problem given in appendix A. Surface loading in the form of a plane time-harmonic wave is considered.

2. Statement of the problem

Consider antisymmetric deformation of an elastic layer of thickness $2h$ ($-\infty \le x_1, x_2 \le \infty$, $-h \le x_3 \leqslant h$) subject to prescribed normal stresses $\pm\frac{1}{2}P(x_1, x_2, t)$ at faces $x_3 = \pm h$ (figure 1), starting from shortened forms of 3D dynamic equations in linear elasticity exposed, in particular, in [7,8,21]; in this section, we use the results of these publications without further reference to them.

Let us first write down the 2D equations governing the long-wave low-frequency approximations, for which

$$L \gg h \quad \text{and} \quad T \gg \sqrt{\frac{\rho}{E}}h, \tag{2.1}$$

where L and T are the typical wavelength and time scale, respectively, E is Young's modulus and ρ is the mass density.

It is well known that the leading-order long-wave low-frequency approximation corresponds to the classical Kirchhoff theory for plate bending resulting in the fourth-order parabolic equation

$$D\Delta^2 w + 2\rho h\frac{\partial^2 w}{\partial t^2} = P, \tag{2.2}$$

where $w(x_1, x_2, t)$ is the vertical displacement of the midplane $x_3 = 0$, t is time, $\Delta = \partial^2/\partial x_1^2 + \partial^2/\partial x_2^2$ is the 2D Laplacian in variables x_1 and x_2, and the bending stiffness D is given by

$$D = \frac{2Eh^3}{3(1-\nu^2)},$$

with ν denoting Poisson's ratio. At $P = 0$ we have from equation (2.2)

$$\frac{T}{h}\sqrt{\frac{E}{\rho}} \sim \frac{L^2}{h^2}. \tag{2.3}$$

We suppose that this condition also holds at $P \neq 0$, unless stated otherwise. Therefore, we may operate with a single small geometric parameter $\eta = h/L \ll 1$.

At next order, we have the refined equation

$$D\Delta^2 w + 2\rho h\left(1 + h^2\frac{7\nu - 17}{15(1-\nu)}\Delta\right)\frac{\partial^2 w}{\partial t^2} = \left(1 - h^2\frac{8-3\nu}{10(1-\nu)}\Delta\right)P, \tag{2.4}$$

where the extra terms in brackets are of order $O(\eta^2)$, cf. (2.2).

Simultaneouly, we rely here on the asymptotic formulation for the Rayleigh wave, which, in contrast with (2.1), is valid at

$$L \ll h \quad \text{and} \quad T \ll \sqrt{\frac{\rho}{E}}h. \tag{2.5}$$

At leading order, this is given by a 2D hyperbolic equation along each of the faces $x_3 = \pm h$; owing to the symmetry of the problem, below we consider only the upper face $x_3 = h$. In terms of the boundary value of the longitudinal wave potential $\Phi(x_1, x_2, x_3, t)$ (e.g. [31]), we have

$$\Delta\Phi_h - \frac{1}{c_{\mathrm{R}}^2}\frac{\partial^2\Phi_h}{\partial t^2} = -\frac{(1+k_2^2)P}{4\mu B}, \tag{2.6}$$

where $\Phi_h = \Phi(x_1, x_2, h, t)$, μ is the Lamé elastic modulus, c_{R} is the Rayleigh wave speed and

$$B = \frac{k_1}{k_2}(1-k_1^2) + \frac{k_2}{k_1}(1-k_2^2) - (1-k_2^4).$$

In the above $k_i = \sqrt{1 - c_{\mathrm{R}}^2/c_i^2}$, $i = 1, 2$, with c_i denoting the longitudinal and shear wave speeds. This equation is initially oriented to near-resonant loading, implementing

$$\Delta P - \frac{1}{c_{\mathrm{R}}^2}\frac{\partial^2 P}{\partial t^2} \ll \frac{P}{L^2}, \tag{2.7}$$

but also handles the Rayleigh wave contribution to the general dynamic response. Condition (2.7), for example, holds for a plane harmonic wave with wavelength L and phase velocity close to c_{R}.

Over the interior ($|x_3| < h$) longitudinal potential $\Phi(x_1, x_2, x_3, t)$ satisfies the 'static' elliptic equation

$$\frac{\partial^2\Phi}{\partial x_3^2} + k_1^2\Delta\Phi = 0, \tag{2.8}$$

whereas a pair of shear potentials $\Psi_i(x_1, x_2, x_3, t)$, $i = 1, 2$, may be found from the boundary value problem

$$\frac{\partial^2\Psi_i}{\partial x_3^2} + k_2^2\Delta\Psi_i = 0, \tag{2.9}$$

with

$$\left.\frac{\partial\Psi_i}{\partial x_3}\right|_{x_3=h} = \frac{1+k_2^2}{2}\frac{\partial\Phi_h}{\partial x_i}. \tag{2.10}$$

Hyperbolic equation (2.6) may also be rewritten through the displacements of the upper face $u_n(x_1, x_2, t)$, $n = 1, 2, 3$. To this end, we express the solutions of elliptic equations (2.8) and (2.9) as

$$\Phi = \Phi_h\, \mathrm{e}^{\sqrt{-\Delta}k_1(x_3-h)} \quad \text{and} \quad \Psi_i = \Psi_{ih}\, \mathrm{e}^{\sqrt{-\Delta}k_2(x_3-h)}, \tag{2.11}$$

where $\sqrt{-\Delta}$ is a 2D pseudo-differential operator and $\Psi_{ih} = \Psi_i(x_1, x_2, h, t)$. Then, taking into account boundary condition (2.10) and also the relation

$$\left.\frac{\partial\Phi}{\partial x_3}\right|_{x_3=h} = -\frac{1+k_2^2}{2}\left(\frac{\partial\Psi_{1h}}{\partial x_1} + \frac{\partial\Psi_{2h}}{\partial x_2}\right), \tag{2.12}$$

we obtain

$$u_i = \left.\frac{\partial\Psi_i}{\partial x_3}\right|_{x_3=h} - \frac{\partial\Phi_h}{\partial x_i} = -\frac{1-k_2^2}{2}\frac{\partial\Phi_h}{\partial x_i}, \quad i = 1, 2 \tag{2.13}$$

and

$$u_3 = \left.\frac{\partial\Phi}{\partial x_3}\right|_{x_3=h} + \frac{\partial\Psi_{1h}}{\partial x_1} + \frac{\partial\Psi_{2h}}{\partial x_2} = \frac{k_1(1-k_2^2)}{1+k_2^2}\sqrt{-\Delta}\Phi_h. \tag{2.14}$$

Finally, with the help of these formulae, we transform (2.6) to the form

$$\Delta u_i - \frac{1}{c_{\mathrm{R}}{}^2}\frac{\partial^2 u_i}{\partial t^2} = -\frac{(1-k_2^4)}{8\mu B}\frac{\partial P}{\partial x_i}, \quad i = 1, 2 \tag{2.15}$$

or

$$\Delta u_3 - \frac{1}{c_R^2}\frac{\partial^2 u_3}{\partial t^2} = -\frac{k_1(1-k_2^2)}{4\mu B}\sqrt{-\Delta}P. \tag{2.16}$$

It is remarkable that the last equation contains the pseudo-differential operator $\sqrt{-\Delta}$ acting on the prescribed stress. Such a form of the equation of motion does not seem to be traditional in solid mechanics.

Similar to the Rayleigh wave equations (2.15) and (2.16), the plate bending equation (2.4) can also be rewritten in terms of the displacements at the upper face $x_3 = h$ starting from the relations

$$u_i = \mathcal{L}_i\frac{\partial w}{\partial x_i} \quad \text{and} \quad u_3 = \mathcal{L}_3 w, \quad i = 1,2, \tag{2.17}$$

where differential operators $\mathcal{L}_i$ and $\mathcal{L}_3$ are defined as

$$\mathcal{L}_i = -h\left\{1 + h^2\left(\frac{\nu+4}{6(1-\nu)}\frac{\partial^2}{\partial x_i^2} - \frac{5\nu}{6(1-\nu)}\frac{\partial^2}{\partial x_j^2}\right)\right\}, \quad i,j = 1,2,\ i \neq j$$

and

$$\mathcal{L}_3 = 1 + h^2\frac{\nu}{2(1-\nu)}\Delta. \tag{2.18}$$

Acting with (2.18) on (2.4) and neglecting $O(\eta^4)$ terms, we get

$$\begin{aligned} &D\Delta^2 u_i + 2\rho h\left(1 + h^2\frac{7\nu-17}{15(1-\nu)}\Delta\right)\frac{\partial^2 u_i}{\partial t^2} \\ &\quad = -h\left\{1 + h^2\left(\frac{\nu+4}{6(1-\nu)}\frac{\partial^2}{\partial x_i^2} - \frac{5\nu}{6(1-\nu)}\frac{\partial^2}{\partial x_j^2} - \frac{8-3\nu}{10(1-\nu)}\Delta\right)\right\}\frac{\partial P}{\partial x_i} \end{aligned} \tag{2.19}$$

and

$$D\Delta^2 u_3 + 2\rho h\left(1 + h^2\frac{7\nu-17}{15(1-\nu)}\Delta\right)\frac{\partial^2 u_3}{\partial t^2} = \left(1 - h^2\frac{4}{5}\Delta\right)P. \tag{2.20}$$

It is obvious that within the Kirchhoff theory we just need to neglect $O(\eta^2)$ terms in all formulae (2.17)–(2.20).

Our goal is to establish 2D composite wave models containing plate bending and Rayleigh wave equations as their asymptotic long-wave low-frequency and short-wave high-frequency limits corresponding to (2.1) and (2.5), respectively. At the same time, we cannot expect such composite models to be able to pick up the asymptotic behaviour of the original 3D problem within the intermediate range

$$L \sim h \quad \text{and} \quad T \sim \sqrt{\frac{\rho}{E}}h. \tag{2.21}$$

This assumption agrees with the general idea of composite equations originally formulated in [29] (see also [30]), not excluding the possibility of asymptotically non-uniform composite theories.

3. Dispersion analysis

It appears to be natural to begin with the analysis of dispersion relations. To this end, we study the plane travelling wave solutions to the homogeneous equations ($P = 0$) in the previous section in the form $\exp[\mathrm{i}(kx_1 - \omega t)]$ with angular frequency ω and wave number k. In this case, the typical

wavelength and time scale are defined as $L \sim k^{-1}$ and $T \sim \omega^{-1}$. First, we substitute the travelling wave solution into equations (2.2) and (2.6) at $P = 0$, having

$$K^4 - \frac{3(1-\nu)}{2}\Omega^2 = 0 \tag{3.1}$$

and

$$K^2 - \frac{\Omega^2}{v_R^2} = 0, \tag{3.2}$$

where

$$K = kh \quad \text{and} \quad \Omega = \frac{\omega h}{c_2}, \tag{3.3}$$

with $v_R = c_R/c_2$ denoting the dimensionless Rayleigh wave speed.

It is obvious that the problem of constructing composite relations does not have a unique solution. Here, by inspecting (3.1) and (3.2), we may readily suggest a very simple composite dispersion relation given by

$$K^4 - \frac{3(1-\nu)}{2}\Omega^2 - \frac{\Omega^4}{v_R^4} = 0. \tag{3.4}$$

At the long-wave low-frequency limit, in which $\Omega \sim K^2$, the last term on the right-hand side of (3.4) is of order $O(\eta^2)$ and may be ignored at leading order, since $\eta = K \ll 1$. Therefore, we arrive at dispersion relation (3.1). On the contrary, at the Rayleigh wave limit ($\Omega \sim K \gg 1$) we may neglect the middle term, which is of order $O(K^{-2})$, arriving at another shortened dispersion relation (3.2).

Next, we obtain a refined composite dispersion relation combining (3.2) with

$$K^4 - \frac{3(1-\nu)}{2}(1 - \delta K^2)\Omega^2 = 0, \tag{3.5}$$

where

$$\delta = \frac{7\nu - 17}{15(1-\nu)}. \tag{3.6}$$

Approximate formula (3.5) arises from the homogeneous refined plate equation (2.4). The sought for composite relation may be written as

$$K^4 - \frac{3(1-\nu)}{2}(1 - \delta K^2)\Omega^2 + \gamma K^2 \Omega^2 \left(K^2 - \frac{\Omega^2}{v_R^2}\right) = 0, \tag{3.7}$$

where γ is a constant parameter to be found. Expressing from this equation K^2 we have

$$K^2 = \frac{1}{2(1+\gamma\Omega^2)}\left\{-\left(\frac{3(1-\nu)\delta}{2} - \gamma\frac{\Omega^2}{v_R^2}\right)\Omega^2 + \right.$$
$$\left. + \sqrt{\left(\frac{3(1-\nu)\delta}{2} - \gamma\frac{\Omega^2}{v_R^2}\right)^2 \Omega^4 + 6(1-\nu)(1+\gamma\Omega^2)\Omega^2}\right\}. \tag{3.8}$$

The latter may be expanded at $\Omega \ll 1$, leading to

$$K^4 = \frac{3(1-\nu)}{2}\Omega^2\left\{1 + \sqrt{\frac{3(1-\nu)}{2}}\delta\Omega + \left(\frac{3\delta^2(1-\nu)}{4} - \gamma\right)\Omega^2 + \cdots\right\}. \tag{3.9}$$

Now, we require the last formula to coincide with the asymptotic expansion of the Rayleigh–Lamb dispersion equation for the bending mode

$$D_{RL}(K, \Omega) = 0, \tag{3.10}$$

with D_{RL} given by (A 7) in appendix A; see considerations in [8, section 7.5]. As a result we have

$$\gamma = \frac{422 - 424\nu - 33\nu^2}{1050(1-\nu)}. \tag{3.11}$$

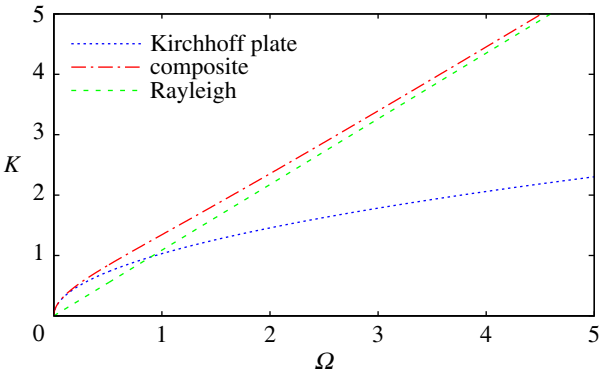

Figure 2. Dispersion curves for Kirchhoff equation (3.1), composite equation (3.4) and Rayleigh wave (3.2).

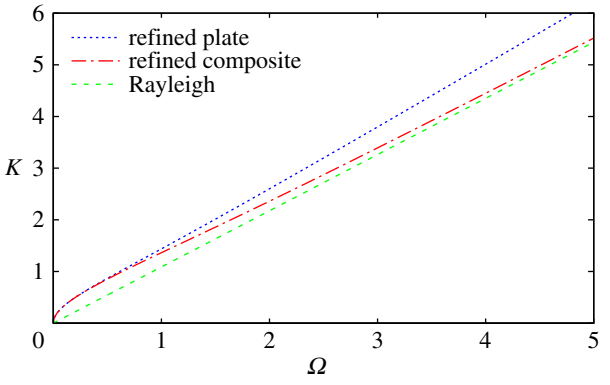

Figure 3. Dispersion curves for refined plate equation (3.5), refined composite equation (3.7) and Rayleigh wave (3.2).

It might easily be verified that at $\Omega \sim K^2 \ll 1$ formula (3.7) to within $O(\eta^4)$ coincides with dispersion relation (3.5), corresponding to the refined plate equation (2.4). As above, neglecting the $O(K^{-2})$ terms, we arrive at (3.2) at the Rayleigh wave limit.

Numerical illustrations are presented in figures 2–4 and table 1 for Poisson's ratio $\nu = 0.25$, for which the positive root of the Rayleigh equation is given, approximately, by $v_R = 0.9194$. Figure 2 displays the dispersion curves for relations (3.1), (3.2) and (3.4) plotted by the dotted, dashed and dash-dotted lines, respectively. Graphic material in this figure is supported by the numerical data in the first, third and fourth columns of table 1. The dispersion curves, plotted in figure 3 by the dotted and dash-dotted lines, correspond to the refined plate and composite relations (3.5) and (3.7), respectively; see also columns 2 and 5 in table 1. As might be expected, the deviation between the predictions of the composite relation (3.4) and its refined form (3.7) is more substantial at relatively low frequencies, while it is rather minor at the high-frequency limit. The obvious reason for this is that both composite relations use the same Rayleigh wave asymptote.

The accuracy of composite relations (3.4) and (3.7) is tested in figure 4 by comparison with the numerical solution of the Rayleigh–Lamb equation, see (3.10) with (A 7). Computations for the latter are also presented in the last column of table 1. We plot the relative error expressed in terms of percentages as

$$e_r = \left| \frac{K_{RL} - K}{K_{RL}} \right| \times 100\%, \tag{3.12}$$

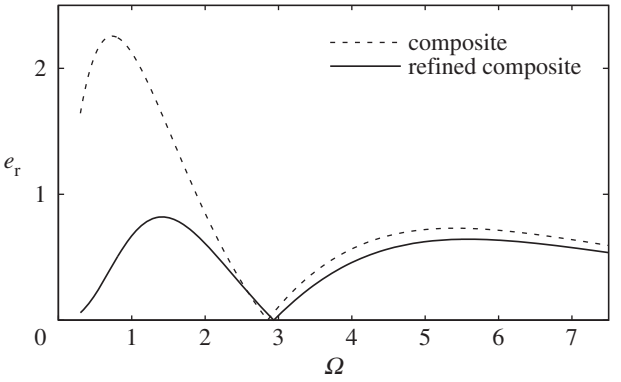

Figure 4. Relative error for composite equation (3.4) and refined composite equation (3.7).

Table 1. Indicative numerical solutions for the exact and approximate dispersion relations.

Ω	Kirchhoff plate dispersion relation (3.1)	refined plate dispersion relation (3.5)	Rayleigh wave asymptote (3.2)	composite dispersion relation (3.4)	refined composite dispersion relation (3.7)	Rayleigh–Lamb dispersion relation (3.10) with (A 7)
0.1	0.3257	0.3376		0.3349	0.3373	0.3373
0.2	0.4606	0.4948		0.4869	0.4930	0.4931
0.3	0.5641	0.6278		0.6131	0.6229	0.6233
0.4	0.6514	0.7506		0.7276	0.7409	0.7418
0.5	0.7282	0.8684		0.8357	0.8520	0.8537
1.0	1.030	1.438		1.344	1.364	1.373
1.5	1.261	2.014		1.845	1.858	1.874
2.0	1.456	2.601		2.355	2.360	2.375
2.5			2.719	2.872	2.872	2.880
3.0			3.263	3.395	3.393	3.391
4.0			4.351	4.454	4.449	4.429
5.0			5.438	5.522	5.517	5.483
6.0			6.526	6.597	6.592	6.550
8.0			8.701	8.755	8.751	8.707
10.0			10.88	10.92	10.92	10.88
11.0			11.96	12.00	12.00	11.97
12.0			13.05	13.09	13.08	13.05

where K_{RL} denotes the associated Rayleigh–Lamb root. It is depicted with dashed and solid lines for K found from the composite relations (3.4) and (3.7), respectively. The curves corresponding to composite relations meet that for the Rayleigh–Lamb equation at $\Omega \approx 3$. This reduces the approximation error over the intermediate frequency range, which is our main concern from the very beginning. To the left of this value, the refined relation has a clear advantage, while to the right of it the difference between (3.4) and (3.7) is not that significant.

4. Composite equations

Motivated by the composite dispersion relation (3.4), we obtain for vertical displacement u_3 along the faces

$$D\Delta^2 u_3 - \frac{D}{c_{\mathrm{R}}^2}\Delta\frac{\partial^2 u_3}{\partial t^2} + 2\rho h\frac{\partial^2 u_3}{\partial t^2} = \left(1 - h^3\frac{k_1(1-k_2^2)}{3B(1-\nu)}\sqrt{-\Delta}\Delta\right)P, \tag{4.1}$$

starting from inhomogeneous equations (2.2) (written in terms of u_3) and (2.16). This simplest composite equation can easily be reduced to the original shortened equations at the long-wave low-frequency and Rayleigh wave limits. First, we scale the original variables in (4.1), setting

$$x_i = \xi_i L, \quad i = 1, 2, \quad \text{and} \quad t = T\tau. \tag{4.2}$$

Then, assuming that $\eta = h/L \ll 1$ and $T = L/\eta c_2$ (see (2.1) and (2.3)), we have

$$\left(\Delta_* - \eta^2\frac{1}{v_{\mathrm{R}}^2}\frac{\partial^2}{\partial\tau^2}\right)\Delta_* u_3 + \frac{3(1-\nu)}{2}\frac{\partial^2 u_3}{\partial\tau^2} = \left(1 + \eta^3\frac{k_1(1-k_2^2)}{3B(1-\nu)}\sqrt{-\Delta_*}\Delta_*\right)\frac{PL^4}{D}, \tag{4.3}$$

where $\Delta_* = \partial^2/\partial\xi_1^2 + \partial^2/\partial\xi_2^2$. It is obvious that, to within the error $O(\eta^2)$, the last equation coincides with the classical Kirchhoff equation (2.2) rewritten in a dimensionless form.

Now let $\eta = h/L \gg 1$ and $T = L/c_{\mathrm{R}}$ (see (2.5)), resulting in the following transformation of composite equation (4.1):

$$\begin{aligned}&\Delta_*\left(\Delta_* u_3 - \frac{\partial^2 u_3}{\partial\tau^2}\right) + \frac{3(1-\nu)}{2}v_{\mathrm{R}}^2\eta^{-2}\frac{\partial^2 u_3}{\partial\tau^2}\\ &\quad = \left(\eta^{-3} + \frac{k_1(1-k_2^2)}{3B(1-\nu)}\sqrt{-\Delta_*}\Delta_*\right)\frac{PL^4\eta^3}{D}.\end{aligned} \tag{4.4}$$

Neglecting $O(\eta^{-2})$ terms and then cancelling out the operator Δ_*, we obtain a dimensionless counterpart of equation (2.16). It can also be verified that the dispersion relation associated with the derived composite equation coincides with dispersion relation (3.4).

Similarly, starting from the leading-order form of (2.19), for which the h^2 terms in both brackets are neglected, and (2.15), we have composite equations written through tangential displacements u_i at the upper face. They are

$$D\left(\Delta - \frac{1}{c_{\mathrm{R}}^2}\frac{\partial^2}{\partial t^2}\right)\Delta u_i + 2\rho h\frac{\partial^2 u_i}{\partial t^2} = -h\left(1 + h^2\frac{1-k_2^4}{6B(1-\nu)}\Delta\right)\frac{\partial P}{\partial x_i}, \quad i = 1, 2. \tag{4.5}$$

Next, we implement the refined plate equation (2.20) and proceed in the same manner as above. Then, a more sophisticated composite equation for vertical displacement may be presented as

$$\begin{aligned}&D\left(1 - h^2\frac{\gamma}{c_2^2}\frac{\partial^2}{\partial t^2}\right)\Delta^2 u_3 + 2\rho h\left(1 + h^2\delta\Delta + h^4\frac{2\gamma}{3(1-\nu)c_{\mathrm{R}}^2}\Delta\frac{\partial^2}{\partial t^2}\right)\frac{\partial^2 u_3}{\partial t^2}\\ &\quad = \left(1 - h^2\frac{4}{5}\Delta + \frac{h^5}{c_2^2}\frac{\gamma k_1(1-k_2^2)}{3B(1-\nu)c_2^2}\sqrt{-\Delta}\Delta\frac{\partial^2}{\partial t^2}\right)P.\end{aligned} \tag{4.6}$$

Again, using proper scalings, it may be shown that equation (4.6) is reduced to its original shortened forms at the long-wave low-frequency and Rayleigh wave limits. In particular, at the low-frequency limit, it takes the form

$$\begin{aligned}&\left(1 - \eta^4\gamma\frac{\partial^2}{\partial\tau^2}\right)\Delta_*^2 u_3 + \frac{3(1-\nu)}{2}\left(1 + \eta^2\delta\Delta_* + \eta^6\frac{2\gamma c_2^2}{3(1-\nu)c_{\mathrm{R}}^2}\Delta_*\frac{\partial^2}{\partial\tau^2}\right)\frac{\partial^2 u_3}{\partial\tau^2}\\ &\quad = \left(1 - \eta^2\frac{4}{5}\Delta_* + \eta^7\frac{\gamma k_1(1-k_2^2)}{3B(1-\nu)}\sqrt{-\Delta_*}\Delta_*\frac{\partial^2}{\partial\tau^2}\right)\frac{PL^4}{D}.\end{aligned} \tag{4.7}$$

This time let us keep the $O(\eta^2)$ terms, neglecting all the smaller ones, to obtain

$$\Delta_*^2 u_3 + \frac{3(1-\nu)}{2}(1+\eta^2\delta\Delta_*)\frac{\partial^2 u_3}{\partial\tau^2} = \left(1-\eta^2\frac{4}{5}\Delta_*\right)\frac{PL^4}{D}. \tag{4.8}$$

This equation is identical to the refined plate equation (2.20) rewritten in dimensionless variables. Now, we get from (4.7) at the Rayleigh wave limit

$$\left(\eta^{-2}-\gamma\frac{c_{\mathrm{R}}^2}{c_2^2}\frac{\partial^2}{\partial\tau^2}\right)\Delta_*^2 u_3 + \frac{c_{\mathrm{R}}^2}{c_2^2}\frac{3(1-\nu)}{2}\left(\eta^{-4}+\eta^{-2}\delta\Delta_* + \frac{2\gamma}{3(1-\nu)}\Delta_*\frac{\partial^2}{\partial\tau^2}\right)\frac{\partial^2 u_3}{\partial\tau^2}$$
$$= \left(\eta^{-5}-\eta^{-3}\frac{4}{5}\Delta_* + \frac{\gamma k_1(1-k_2^2)}{3B(1-\nu)}v_{\mathrm{R}}^2\sqrt{-\Delta_*}\Delta_*\frac{\partial^2}{\partial\tau^2}\right)\frac{PL^4\eta^3}{D}. \tag{4.9}$$

At leading order, the latter becomes

$$\Delta_*\frac{\partial^2}{\partial\tau^2}\left(\Delta_*-\frac{\partial^2}{\partial\tau^2}\right)u_3 = -\frac{L^4\eta^3}{D}\frac{k_1(1-k_2^2)}{3B(1-\nu)}\sqrt{-\Delta_*}\Delta_*\frac{\partial^2 P}{\partial\tau^2}. \tag{4.10}$$

Finally, cancelling out operator $\Delta_*(\partial^2/\partial\tau^2)$, we have the Rayleigh wave equation (2.16) presented in a dimensionless form.

As might be expected, the dispersion relation corresponding to the refined composite equation (4.6) is the same as (3.7).

5. Example

As an example, we consider the effect of the surface loads (figure 1) in the form of plane time-harmonic travelling waves, for which $P = P_0 e^{\mathrm{i}(k_0 x_1-\omega t)}$, where $k_0 = k_0(\omega)$ is a given function of the angular frequency ω, corresponding to the near-resonant excitation, see (2.7). Let us search for the solution to the differential equations in §§2 and 4 also in the form of a plane travelling wave, i.e. take $u_3 = (AhP_0/\mu)\,\mathrm{e}^{\mathrm{i}(k_0 x_1-\omega t)}$, where A is normalized amplitude.

First, insert u_3 and P into composite equation (4.1) and its shortened limiting forms (2.2) and (2.16). Then, we have, respectively,

$$A = \frac{3(1-\nu)B + k_1(1-k_2^2)K_0^3}{4B\left(K_0^4 - \frac{1}{v_{\mathrm{R}}^2}K_0^2\Omega^2 - \frac{3(1-\nu)}{2}\Omega^2\right)}, \tag{5.1}$$

$$A = \frac{3(1-\nu)}{4}\frac{1}{K_0^4 - \dfrac{3(1-\nu)}{2}\Omega^2} \tag{5.2}$$

and

$$A = \frac{k_1(1-k_2^2)}{4B}\frac{K_0}{K_0^2 - \Omega^2/v_{\mathrm{R}}^2}, \tag{5.3}$$

where $K_0 = k_0 h$ and, as before, $\Omega = \omega h/c_2$.

Next, insert u_3 and P into the refined composite and plate equations (4.6) and (2.20) to obtain

$$A = \frac{1}{20B}\frac{3(1-\nu)(5+4K_0^2)B + 5k_1(1-k_2^2)\gamma K_0^3\Omega^2}{(1+\gamma\Omega^2)K_0^4 - [3(1-\nu)/2 - (7\nu-17)K_0^2/10 + \gamma K_0^2\Omega^2/v_{\mathrm{R}}^2]\Omega^2} \tag{5.4}$$

and

$$A = \frac{3(1-\nu)}{20}\frac{5+4K_0^2}{K_0^4 - (3(1-\nu)/2)(1-\delta K_0^2)\Omega^2}, \tag{5.5}$$

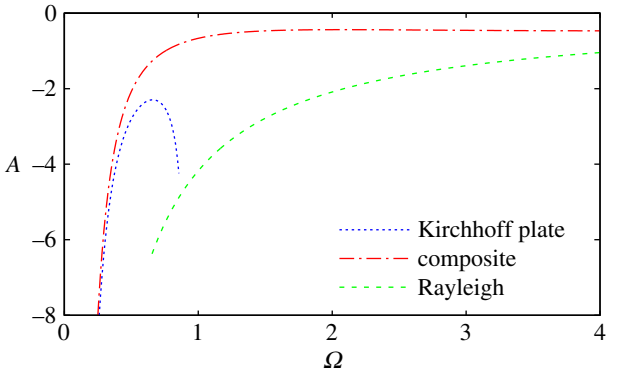

Figure 5. Displacement amplitude A for Kirchhoff equation (5.2), composite equation (5.1) and Rayleigh wave equation (5.3).

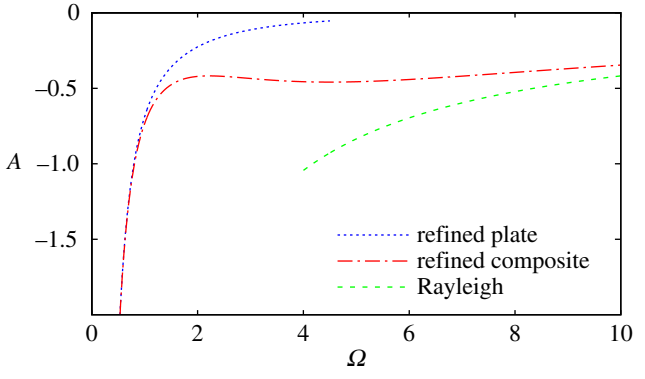

Figure 6. Displacement amplitude A for refined plate equation (5.5), refined composite equation (5.4) and Rayleigh wave equation (5.3).

or, multiplying the numerator and denominator of the latter by $5-4K_0^2$,

$$A=\frac{3(1-\nu)}{20}\,\frac{25-16K_0^4}{5K_0^4-(15/2)(1-\nu)\Omega^2-(5/2)(1+\nu)K_0^2\Omega^2-4K_0^6-6(1-\nu)\delta K_0^4\Omega^2}. \tag{5.6}$$

This formula, to within higher-order terms, coincides with the long-wave low-frequency expansion of the exact solution (A 5) at $K=K_0$, see appendix A. Also, expression (5.3) is the same as the Rayleigh wave limit (A 9) in appendix A at $K=K_0$ due to the identity $4B=v_{\mathrm{R}}R'(v_{\mathrm{R}})$.

Formulae (5.1)–(5.5) are tested at $K_0(\Omega)=(1-\varepsilon)\Omega/v_{\mathrm{R}}$, $\varepsilon\ll 1$, in order to satisfy condition (2.7) underlying the adapted Rayleigh wave model. In this case the $O(K_0^6)$ terms in the denominator of (5.6) may be ignored; these are essential under assumption $\Omega\sim K_0^2$ (see also (2.3)), characteristic of free bending vibration.

Numerical data are given in figures 5–7 and table 2 for $\nu=0.25$ and $\varepsilon=0.02$. In figures 5 and 6, the solutions of composite equations (5.1) and (5.4) are plotted by the dash-dotted line, along with those of plate equations (5.2) and (5.5) by the dotted line, and the Rayleigh wave model (5.3) by the dashed line. It is worth noting that the behaviours of the solutions of the Kirchhoff and refined plate equations appear to be quite different over the intermediate frequency range.

In figure 7, the solutions of the composite equations are compared with the exact solution of the associated problem in plane elasticity (A 5); see also the last column in table 2. The graphs for (5.1), (5.4) and (A 5) are drawn with dotted, dashed and solid lines, respectively. Figure 7 and table 2 indicate a reasonable accuracy of the composite equations over the intermediate frequency range, where they are not asymptotic. As for the dispersion curves in §3, the main improvement brought about by the refined composite equation is observed at relatively low frequencies.

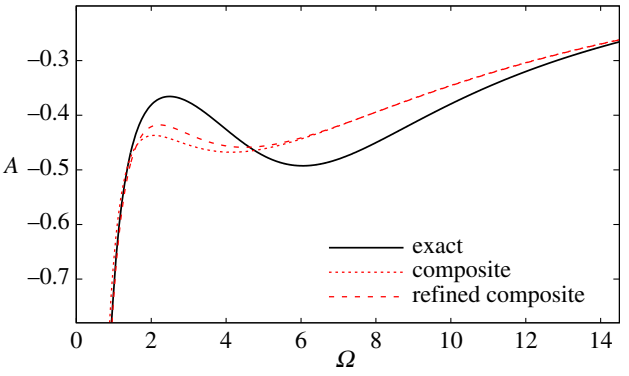

Figure 7. Displacement amplitude A for composite equation (5.1), refined composite equation (5.4) and plane elasticity (A 5).

Table 2. Numerical values of displacement amplitude A.

Ω	Kirchhoff equation (5.2)	refined plate equation (5.5)	Rayleigh wave equation (5.3)	composite equation (5.1)	refined composite equation (5.4)	plane elasticity equations (A 5)
0.1	−50.58	−50.26		−50.00	−50.26	−50.20
0.2	−13.10	−12.75		−12.52	−12.75	−12.70
0.3	−6.195	−5.805		−5.591	−5.806	−5.759
0.4	−3.828	−3.368		−3.180	−3.371	−3.330
0.5	−2.804	−2.235		−2.074	−2.242	−2.206
1.0	3.391	−0.6853		−0.6660	−0.7320	−0.7159
1.5	0.1405	−0.3593		−0.4686	−0.4762	−0.4549
2.0	0.0348	−0.2254		−0.4373	−0.4210	−0.3811
2.5			−1.670	−0.4429	−0.4211	−0.3657
3.0			−1.392	−0.4546	−0.4348	−0.3759
4.0			−1.044	−0.4675	−0.4562	−0.4260
5.0			−0.8350	−0.4616	−0.4564	−0.4741
6.0			−0.6958	−0.4435	−0.4415	−0.4925
8.0			−0.5219	−0.3942	−0.3944	−0.4502
10.0			−0.4175	−0.3455	−0.3460	−0.3794
11.0			−0.3795	−0.3237	−0.3242	−0.3478
12.0			−0.3479	−0.3038	−0.3043	−0.3201

6. Conclusion

Composite wave models for thin elastic plates are established, benefiting from the hyperbolic equation for the Rayleigh wave as their short-wave limiting form. The numerical results for the free and forced vibrations, presented in the paper, demonstrate a reasonable accuracy of the proposed 2D equations over the intermediate frequency range, where they are not asymptotic. As might be expected, the refined composite equation (4.6) corresponding to the higher-order long-wave approximation (2.4) is more accurate than the simple composite equation (4.1) at low frequencies. The composite theories might also be refined over the high-frequency range by using a high-order approximation for the Rayleigh wave, which is however not yet available. We also

remark that conditions (2.3) and (2.7) on the surface loading can generally be relaxed as has been done in the example in §5 for assumption (2.3).

The developed models, as any 2D formulation, do not reproduce all the features of the original 3D problem. In particular, they only pretend to approximate the fundamental antisymmetric Rayleigh–Lamb mode, which is nevertheless of the most interest for modelling the surface loading, exciting both bending and Rayleigh waves over low- and high-frequency bands, respectively. Preserving both the low- and high-frequency components of the surface loading on the right-hand sides of composite equations (4.1), (4.5) and (4.6) appears to be a non-trivial feature of the presented framework.

It is obvious that the problem of constructing a composite equation does not have a unique solution. At the same time, it is intuitively clear that equations (4.1), (4.5) and (4.6), involving, respectively, just the fourth- and sixth-order derivatives, are optimal in a sense. Of course, we cannot expect them to lead immediately to composite expansions not only along the faces but also over the interior of the plate. In this case, polynomial approximations across the thickness typical for asymptotic plate theories have to be matched with exponentially decaying surface wave fields.

Another challenge is concerned with the formulation of the initial and boundary conditions. In particular, the long-wave procedure in [32] should be adapted for incorporating the short-wave behaviour. The derivation of the boundary conditions apparently has to refer to the results of [33], in which the reflection of the Rayleigh wave from a corner was studied.

For the sake of simplicity, we analysed a specific loading along both plate faces as shown in figure 1 in order to deal with the antisymmetric deformation only. Within a more general set-up, the symmetric fundamental mode is excited as well. For the latter, similar composite equations may also be established. Moreover, there is a potential for a composite wave theory for thin elastic shells due to a non-significant curvature effect on short-wave motions.

Data accessibility. The article has no additional data.

Authors' contributions. All authors have contributed equally to the paper.

Competing interests. The authors have no competing interests.

Funding. The research of B.E. and M.P. is supported by the Scientific Projects of Anadolu University, grant no. 1408F370.

Acknowledgements. B.E. and J.K. acknowledge the financial support of TÜBİTAK via the 2221 - Fellowships for Visiting Scientists and Scientists on Sabbatical Leave.

Appendix A. Exact solution of the plane time-harmonic problem

The governing equations in plane elasticity are given by (see [31])

$$\Delta\varphi - \frac{1}{c_1^2}\frac{\partial^2\varphi}{\partial t^2} = 0 \quad \text{and} \quad \Delta\psi - \frac{1}{c_2^2}\frac{\partial^2\psi}{\partial t^2} = 0, \tag{A 1}$$

where $\varphi(x_1, x_3, t)$ and $\psi(x_1, x_3, t)$ are wave potentials, and c_1 and c_2 are longitudinal and shear wave speeds given, respectively, by

$$c_1 = \sqrt{\frac{E(1-\nu)}{(1+\nu)(1-2\nu)\rho}} \quad \text{and} \quad c_2 = \sqrt{\frac{E}{2(1+\nu)\rho}}.$$

Consider a layer ($-\infty \le x_1 \le \infty$, $-h \le x_3 \le h$) with the boundary conditions on its faces $x_3 = \pm h$ given in terms of wave potentials by

$$\mu\left(\frac{\partial^2\psi}{\partial x_1^2} - \frac{\partial^2\psi}{\partial x_3^2} + 2\frac{\partial^2\varphi}{\partial x_1 \partial x_3}\right)\bigg|_{x_3=\pm h} = 0 \tag{A 2}$$

and

$$\frac{\mu}{\chi^2}\left(\frac{\nu}{1-\nu}\frac{\partial^2\varphi}{\partial x_1^2} + \frac{\partial^2\varphi}{\partial x_3^2} + 2\chi^2\frac{\partial^2\psi}{\partial x_1 \partial x_3}\right)\bigg|_{x_3=\pm h} = \pm\frac{P_0}{2}e^{i(kx_1-\omega t)}, \tag{A 3}$$

where $\chi = c_2/c_1$.

The solution to the formulated problem for the vertical displacement at the faces,

$$u_3 = \left(\frac{\partial \varphi}{\partial x_3} + \frac{\partial \psi}{\partial x_1}\right)\Big|_{x_3=\pm h}, \tag{A 4}$$

takes the form $u_3 = (AhP_0/\mu)\,\mathrm{e}^{\mathrm{i}(kx_1-\omega t)}$ with

$$A = -\frac{\alpha \Omega^2}{D_{\mathrm{RL}}}, \tag{A 5}$$

where

$$\alpha = \sqrt{K^2 - \chi^2\Omega^2} \quad \text{and} \quad \beta = \sqrt{K^2 - \Omega^2} \tag{A 6}$$

and the Rayleigh–Lamb denominator is written as

$$D_{\mathrm{RL}}(K, \Omega) = (K^2 + \beta^2)^2 \tanh\alpha - 4K^2\alpha\beta \tanh\beta, \tag{A 7}$$

with Ω and K defined by (3.3).

The long-wave low-frequency expansion of formula (A 5) at $\Omega \ll 1$ and $K \ll 1$ reads as

$$A = \frac{3(1-\nu)}{4} \frac{1}{K^4 - (4/5)K^6 - (3/2)(1-\nu)\Omega^2 - (1/2)(1+\nu)K^2\Omega^2 + \cdots}. \tag{A 8}$$

At leading order, we have for the Rayleigh wave contribution at $K \sim \Omega \gg 1$, and $|\Omega/K - v_{\mathrm{R}}| \ll 1$ (see (2.7)),

$$A = \frac{1}{4K} \frac{v_{\mathrm{R}}^2\sqrt{1 - \chi^2 v_{\mathrm{R}}^2}}{R'(v_{\mathrm{R}})(c^2 - v_{\mathrm{R}}^2)}, \tag{A 9}$$

where $c = \Omega/K$, and the Rayleigh denominator is given by

$$R(c) = (2 - c^2)^2 - 4\sqrt{1 - \chi^2 c^2}\sqrt{1 - c^2}, \tag{A 10}$$

with prime denoting a differentiation with respect to the argument of the Rayleigh denominator.

References

1. Chebakov R, Kaplunov J, Rogerson GA. 2017 A non-local asymptotic theory for thin elastic plates. *Proc. R. Soc. A* **473**, 20170249. (doi:10.1098/rspa.2017.0249)
2. Pradhan SC, Phadikar JK. 2009 Nonlocal elasticity theory for vibration of nanoplates. *J. Sound Vib.* **325**, 206–223. (doi:10.1016/j.jsv.2009.03.007)
3. Lu P, Zhang PQ, Lee HP, Wang CM, Reddy JN. 2007 Non-local elastic plate theories. *Proc. R. Soc. A* **463**, 3225–3240. (doi:10.1098/rspa.2007.1903)
4. Sajadi B, Goosen H, van Keulen F. 2017 Capturing the effect of thickness on size-dependent behavior of plates with nonlocal theory. *Int. J. Solids Struct.* **115–116**, 140–148. (doi:10.1016/j.ijsolstr.2017.03.010)
5. Ebrahimi F, Barati MR, Dabbagh A. 2016 A nonlocal strain gradient theory for wave propagation analysis in temperature-dependent inhomogeneous nanoplates. *Int. J. Eng. Sci.* **107**, 169–182. (doi:10.1016/j.ijengsci.2016.07.008)

6. Bers L, John F, Schechter M. 1964 *Partial differential equations*. Lecture Notes in Applied Mathematics. Providence, RI/New York, NY: AMS, John Wiley and Sons.
7. Goldenveizer AL, Kaplunov JD, Nolde EV. 1993 On Timoshenko-Reissner type theories of plates and shells. *Int. J. Solids Struct.* **30**, 675–694. (doi:10.1016/0020-7683(93)90029-7)
8. Kaplunov JD, Kossovich LYu, Nolde EV. 1998 *Dynamics of thin walled elastic bodies*. London, UK: Academic Press.
9. Goldenveizer AL, Kaplunov YuD, Nolde EV. 1990 Asymptotic analysis and improvements of Timoshenko–Reissner-type theories of plates and shells. *Mechanics of Solids* (*Izv. AN SSSR, Mekhanika Tverdogo Tela*) **25**, 126–139.
10. Metrikine AV. 2006 On causality of the gradient elasticity models. *J. Sound Vib.* **297**, 727–742. (doi:10.1016/j.jsv.2006.04.017)
11. Metrikine AV, Askes H. 2002 One-dimensional dynamically consistent gradient elasticity models derived from a discrete microstructure. *Eur. J. Mech. A/Solids* **21**, 555–572. (doi:10.1016/s0997-7538(02)01218-4)
12. Askes H, Metrikine AV, Pichugin AV, Bennett T. 2008 Four simplified gradient elasticity models for the simulation of dispersive wave propagation. *Philos. Mag.* **88**, 3415–3443. (doi:10.1080/14786430802524108)
13. Craster RV, Joseph LM, Kaplunov J. 2014 Long-wave asymptotic theories: the connection between functionally graded waveguides and periodic media. *Wave Motion* **51**, 581–588. (doi:10.1016/j.wavemoti.2013.09.007)
14. Grigolyuk EI, Selezov IT. 1973 *Nonclassical theories of vibrations of rods, plates and shells*. Advances in Sciences and Technology, Ser. Mechanics of Deformable Solids, vol. 5. Moscow, Russia: VINITI. [In Russian.]
15. Elishakoff I, Kaplunov J, Nolde E. 2015 Celebrating the centenary of Timoshenko's study of effects of shear deformation and rotary inertia. *Appl. Mech. Rev.* **67**, 60802. (doi:10.1115/1.4031965)
16. Selezov I. 1999 Some hyperbolic models for wave propagation. In *Hyperbolic problems: theory, numerics, applications* (eds M Fey, R Jeltsch). International Series of Numerical Mathematics, vol. 130, pp. 833–842. Basel, Switzerland: Birkhäuser.
17. Selezov IT. 1994 Hyperbolic models of wave propagation in rods, plates and shells. *Mechanics of Solids* (*Izv. RAN, Mekhanika Tverdogo Tela*) **29**, 64–77.
18. Le KC. 2012 *Vibrations of shells and rods*. Berlin, Germany: Springer Science & Business Media.
19. Kossovich LYu. 1986 *Nonstationary problems of the theory of elastic thin shells*. Saratov, Russia: Saratov University Press.
20. Kaplunov J, Prikazchikov DA. 2013 Explicit models for surface, interfacial and edge waves. In *Dynamic localization phenomena in elasticity, acoustics and electromagnetism* (eds RV Craster, J Kaplunov). CISM Courses and Lectures, vol. 547, pp. 73–114. Vienna, Austria: Springer.
21. Kaplunov J, Prikazchikov DA. 2017 Asymptotic theory for Rayleigh and Rayleigh-type waves. In *Advances in applied mechanics* (eds SPA Bordas, DS Balint), vol. 50, pp. 1–106. Amsterdam, The Netherlands: Elsevier.
22. Friedlander FG. 1948 On the total reflection of plane waves. *Q. J. Mech. Appl. Math.* **1**, 376–384. (doi:10.1093/qjmam/1.1.376)
23. Chadwick P. 1976 Surface and interfacial waves of arbitrary form in isotropic elastic media. *J. Elast.* **6**, 73–80. (doi:10.1007/BF00135177)
24. Parker DF, Kiselev AP. 2008 Rayleigh waves having generalised lateral dependence. *Q. J. Mech. Appl. Math.* **62**, 19–30. (doi:10.1093/qjmam/hbn022)
25. Parker DF. 2013 The Stroh formalism for elastic surface waves of general profile. *Proc. R. Soc. A* **469**, 20130301. (doi:10.1098/rspa.2013.0301)
26. Ege N, Erbaş B, Prikazchikov DA. 2015 On the 3D Rayleigh wave field on an elastic half-space subject to tangential surface loads. *ZAMM - J. Appl. Math. Mech. / Z. Angew. Math. Mech.* **95**, 1558–1565. (doi:10.1002/zamm.201400211)
27. Kaplunov J, Prikazchikov DA, Erbaş B, Şahin O. 2013 On a 3D moving load problem for an elastic half space. *Wave Motion* **50**, 1229–1238. (doi:10.1016/j.wavemoti.2012.12.008)
28. Erbaş B, Kaplunov J, Prikazchikov DA, Şahin O. 2017 The near-resonant regimes of a moving load in a three-dimensional problem for a coated elastic half-space. *Math. Mech. Solids* **22**, 89–100. (doi:10.1177/1081286514555451)
29. Van Dyke M. 1975 Perturbation methods in fluid mechanics/Annotated edition. NASA STI/Recon Technical Report A. 75. Research supported by the U.S. Air Force. Stanford, CA: Parabolic Press.

30. Andrianov IV, Awrejcewicz J, Manevitch LI. 2013 *Asymptotical mechanics of thin-walled structures*. Berlin, Germany: Springer Science & Business Media.
31. Achenbach J. 2012 *Wave propagation in elastic solids*, vol. 16. Amsterdam, The Netherlands: Elsevier.
32. Kaplunov J, Nolde E, Rogerson GA. 2006 An asymptotic analysis of initial-value problems for thin elastic plates. *Proc. R. Soc. A* **462**, 2541–2561. (doi:10.1098/rspa.2006.1687)
33. Kamotski VV, Fradkin LJ, Samokish BA, Borovikov VA, Babich VM. 2006 On Budaev and Bogy's approach to diffraction by the 2D traction-free elastic wedge. *SIAM. J. Appl. Math.* **67**, 235–259. (doi:10.1137/050637297)